Chemical Physics 171 (1993) 97–106
North-Holland

Solvent effects on the torsional dynamics of a twisted intramolecular charge transfer (TICT) molecule: bianthryl in acetonitrile

Maureen J. Smith, Karsten Krogh-Jespersen and Ronald M. Levy
Department of Chemistry, Rutgers University, New Brunswick, NJ 08903, USA

Received 27 August 1992

Molecular dynamics simulations have been used to study the torsional potential surface and dynamics of 9,9′-bianthryl (BA) in the polar aprotic solvent acetonitrile. In the gas phase, the ground state (S_0) torsional potential has a minimum at the perpendicular conformation with a twist angle of 90°, while for the first excited singlet electronic state (S_1), the 90° twist angle corresponds to a local maximum with symmetric minima located at ≈70° and ≈110°, respectively. The solvent coupling to the torsional coordinate in both the ground and excited states results in increased twisting with respect to the gas phase potential. Two models for the charge distribution in the electronically excited state were studied corresponding to a locally excited (LE) and a charge transfer (CT) state, respectively. The partial atomic charges representative of the S_0, LE, and CT states of BA were obtained from fits to molecular electrostatic potentials created by electronic structure calculations employing the semi-empirical INDO/1S Hamiltonian. The transfer of an electron between the two anthracene rings does not have a large effect on the torsional potential of mean force in acetonitrile. This surprising result is partly attributed to delocalization of the electronic charge occurring over a large molecular region without substantial atomic charge buildup or depletion occurring on any specific atomic site fully exposed to the solvent. The torsional dynamics of bianthryl following photoexcitation was modeled by running nonequilibrium trajectories on the excited state surfaces with initial configurations chosen from the ground state distribution. The relaxation time τ_t for bianthryl on the torsional surface in the excited state is estimated to be between 1.5 and 2 ps in acetonitrile. We have also calculated the time correlation function $C(t)$ for the fluctuations in the bianthryl–acetonitrile electrostatic potential. The relaxation time is estimated to be $\tau_s \approx 200$ fs. The possible consequences of the relation $\tau_s < \tau_t$ are discussed.

1. Introduction

Electronically excited states in aromatic molecules belonging to the special class of twisted intramolecular charge transfer (TICT) compounds have been studied extensively over the past thirty years [1–3]. These molecules exhibit dual fluorescence in polar solution from both locally excited (LE) and charge transfer (CT) excited states. At present, there are over 50 compounds known to form TICT states [2]. A variety of experimental and theoretical methods have been used to examine the TICT mechanism, including photodynamic studies of the kinetics for TICT state formation [1].

One TICT molecule whose excited state fluorescence has been studied both experimentally and theoretically is 9,9′-bianthryl (BA), see fig. 1. Experimental studies have been performed using supersonic beams and laser-induced fluorescence spectroscopy to determine its gas phase torsional potential [4–6]. Other studies have examined the behavior of bianthryl in a wide range of solvents [1,7]. In the gas phase, the ground state torsion of bianthryl has a minimum at the perpendicular conformation 90°,

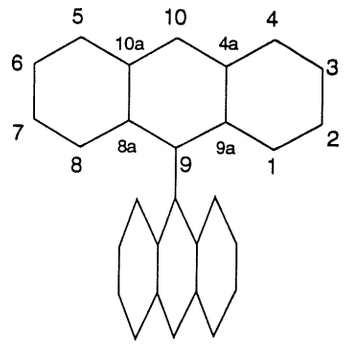

Fig. 1. Diagram of 9,9′-bianthryl.

while the excited state has a double minimum located at $\pm 12°$–$23°$ to either side of a 90° maximum [4–6]. The excited state is exclusively LE in character in the gas phase. In solution, the effective potential for torsional twisting will be modified due to the interactions between bianthryl and the solvent. Furthermore, the LE and CT states are expected to interact very differently with a polar solvent. Experiments indicate that the Stokes red-shift of bianthryl is highly dependent on the solvent polarity [8].

Both outer sphere (solvent dynamics) and inner sphere (torsional twisting) processes have been invoked as rate limiting mechanisms for electron transfer in different TICT molecules. For bianthryl, a theoretical treatment of the steady state absorption and emission spectra, and the time dependent fluorescence, has been based on an adiabatic excited state potential surface [9]. In this phenomenological model, the LE and CT states are strongly coupled, and the charge transfer is assumed to be governed solely by the solvent dynamics. The model fits the experimental data well. However, based on electronic structure arguments, the torsional motion of bianthryl is expected to influence the dynamics of the charge transfer process. At a twist angle of 90°, the intramolecular electron transfer between the π orbitals of the anthracenes is forbidden because the two sets of ring orbitals are orthogonal. Based on orbital overlap considerations, the rate constant for electron transfer is expected qualitatively to increase quadratically with bianthryl twist away from 90°. Assuming that in solution there is also a significant population of 90° conformers in the ground state, whether the charge transfer is controlled by the twisting dynamics or the solvent dynamics depends on the relative rates of the two processes. If the twisting occurs on a time scale that is comparable to or faster than the dielectric relaxation time of the solvent, then the charge transfer should correlate with the "solvation time" of the solvent [7,10–12]. On the other hand, if the twisting is much slower than the solvation time, then a population of bianthryl conformers should remain unreactive on the solvation time scale. Molecular dynamics simulations of bianthryl in solution provide a powerful approach to addressing the problem of the relative time scales of twisting and solvent dynamics. In this connection, we note the long history of the use of molecular dynamics simulations to study the cis–trans photoisomerization solution dynamics of π conjugated systems (polyenes and polyethylene) [13–15].

Equilibrium and nonequilibrium molecular dynamics simulations have been carried out to study the effect of the polar aprotic solvent acetonitrile on the torsional potential surface and torsional dynamics of bianthryl. The simulations have been used to construct effective potentials (potentials of mean force) for the twisting motion in acetonitrile. While the effect of solvent on the torsional potential of nonpolar molecules tends to be small [16,17], there can be quite large solvent effects on the torsional potential of highly polar molecules [18]. Bianthryl presents an interesting case since the ground state corresponds to a nonpolar solute, while in the charge transfer excited state, the molecule is highly polar. We have focused on two questions in this study: (1) how strongly does the acetonitrile solvent couple to the torsional coordinate in the S_0 ground and the S_1 excited states, and (2) what is the time scale for bianthryl to equilibrate on the S_1 surface in acetonitrile following the simulated photoexcitation. The model potential surfaces and molecular dynamics methods used in this study are presented in the following section. The results and discussion are presented in section 3.

2. Methods

Molecular dynamics simulations of a bianthryl solute molecule in a cubic box of 193 acetonitrile molecules were carried out in the *NVT* ensemble using the IMPACT program [19]. The equations of motion were integrated with the velocity Verlet algorithm using the RATTLE algorithm to maintain bond lengths and angles for acetonitrile [20]. The time step was 1 fs. Nonbonded interactions were truncated at 10 Å. The edge length of the box was 26.6 Å and periodic boundary conditions were employed. The model of Jorgensen and Briggs was used for acetonitrile [21]. This model uses an extended atom representation for the methyl group. Partial atomic charges representative of the ground (S_0) and excited (LE, CT) states of BA were obtained from electronic structure calculations employing the semi-empirical INDO/1S model Hamiltonian [22] within the ESPPAC program [23]. Sets of atom centered charges were cre-

ated from fits to quantum mechanical molecular electrostatic potentials according to recently developed procedures described elsewhere [24]. The electrostatic potential is a one-electron property (the expectation value of r^{-1}) and its computation requires the density matrix for the electronic state of interest. For S_0, a Hartree–Fock wavefunction formed the basis for the one-electron reduced density matrix. Since bianthryl in its perpendicular conformation exhibits D_{2d} symmetry, none of the electronic states will possess a permanent, nonzero dipole moment and the charge transfer state is actually more appropriately labeled a charge resonance state at this particular twist angle [25]. Standard configuration interaction procedures were modified in order to develop atomic charges representing the CT state. The excitation space consisted of all possible single excitations derived from the 30 molecular orbitals bracketing the Fermi level (15 "up", 15 "down"). The required density matrix was then created using only those singly excited configurations that represent a unidirectional charge transfer from one anthracene unit to the other unit. The resulting charge distribution thus reflects the complete transfer of one full electron at the perpendicular conformation. The atomic charges derived for S_0 were also used for the nonpolar LE state. This approximation is justified by the fact that BA is an even alternant hydrocarbon and hence there will be no charge rearrangement between ground and excited states to first order within a π-electron only picture. Examination of partial atomic charges for S_0 and LE computed in the zero-differential overlap approximation with our configuration interaction wavefunction justifies this approximation. The largest difference in partial atomic charges between the two states is 2×10^{-2} (C10, C10′) and all other differences are less than 10^{-2}. The partial charges for the S_0, LE, and CT states are listed in table 1. The CT state in the simulation has a dipole moment of 15.6 D directed along the 9,9′-axis.

The dihedral angle about the 9,9′ bond of bianthryl, ϕ, is the twist coordinate which affects the coupling of the LE and CT states. The torsional potential of Yamasaki et al. [6] was used to model the intrinsic molecular contribution to the twisting of the two anthracene rings about the central bond (see fig. 2). These authors parameterized the torsional potentials corresponding to the S_0 and S_1 states from the vibronic bands observed in the laser-induced fluorescence spectrum of BA in a free jet. The potential function was assumed to have the form

$$V_{\mathrm{mol}}(\phi)=\sum_{n=0}^{6}\tfrac{1}{2}V_n(1-\cos n\phi)\ .$$

Fitting to the data [6] gave the following potential parameters (in kcal/mol) for S_0: $V_2=-143.5$, $V_4=-2.00$, $V_6=14.87$ and for S_1: $V_2=-10.4$, $V_4=-3.80$, $V_6=0.0$. The S_1 barrier height is ≈0.4 kcal/mol. In these gas phase experiments the S_1 potential corresponds to the LE state. There is no spectroscopic information available on the gas phase torsional potential of the CT state. However, the twist potential computed by Rettig and Zander [25] for the lowest CT state shows features qualitatively similar to that computed (and experimentally observed) for the LE state. In our simulations we have used the same intrinsic torsional potential parameters to represent both the LE and CT states. That is, in our model the LE and CT states differ only in the partial charges assigned to bianthryl atoms.

The effective torsional potential contains two contributions: the intrinsic molecular potential energy arising from the interactions among the anthracene rings and a solvent term arising from the interactions of bianthryl with the solvent, acetonitrile. In the adiabatic limit where the solvent equilibrates instantaneously to the changes in the bianthryl torsion, the twisting is determined by the torsional potential of mean force $V_{\mathrm{pmf}}(\phi)$. The dihedral potential of mean force is related to the bianthryl dihedral angle distributions calculated from the equilibrium simulations by the following formula:

$$\begin{aligned}V_{\mathrm{pmf}}(\phi)&=-k_{\mathrm{B}}T\ln\rho(\phi)+C\\&=V_{\mathrm{mol}}(\phi)+V_{\mathrm{solvent}}(\phi)\ .\end{aligned}$$

Since the potentials of mean force are only determined by the simulations up to an additive constant, we have chosen the constant in each case so as to align the energy curves at $V(\phi=90°)$ in the figures.

The probability distributions $\rho(\phi)$ corresponding to the S_0, LE and CT states for bianthryl in acetonitrile were calculated from three different simulations. In each simulation, the bianthryl state (S_0, LE or CT) was allowed to equilibrate with solvent for 1 ps. Following equilibration, a production run of 150

Table 1
Bianthryl ground (S_0) and excited (LE, CT) state parameters used in MD simulations

Partial atomic charges

atom	S_0, LE	CT	atom	S_0, LE	CT
C1, C8	−0.1192	−0.1934	H1, H8	0.0529	0.0795
C2, C7	−0.0747	−0.2446	H2, H7	0.0578	0.1059
C3, C6	−0.0291	0.0366	H3, H6	0.0502	0.0017
C4, C5	−0.1717	−0.2526	H4, H5	0.0727	0.0629
C9	−0.1768	−0.4340	H10	0.1187	0.1330
C10	−0.3229	−0.5185	H1′, H8′	0.0529	0.0371
C4a, C10a	0.1601	0.1487	H2′, H7′	0.0578	0.0079
C8a, C9a	0.1915	0.1856	H3′, H6′	0.0502	0.1015
C1′, C8′	−0.1192	−0.0510	H4′, H5′	0.0727	0.0834
C2′, C7′	−0.0747	0.0952	H10′	0.1187	0.0890
C3′, C6′	−0.0291	−0.1107			
C4′, C5′	−0.1717	−0.0788			
C9′	−0.1768	0.1263			
C10′	−0.3229	−0.0830			
C4a′, C10a′	0.1601	0.1856			
C8a′, C9a′	0.1915	0.1431			

Force constants		Equilibrium geometries		Nonbonded Lennard-Jones parameters		
coordinate	value	coordinate	value	atom	σ	ϵ
C–C	469	C–C	1.40	C	1.648	0.12
C–H	340	C–H	1.09	H	1.372	0.01
C–C–C	85	C–C–C	120			
H–C–C	35	H–C–C	120			
C9–C9′	469	C9–C9′	1.45			

ps simulation was carried out with sampling of the torsional coordinate every 10 fs, for a total of 15000 data points contributing to the corresponding probability distribution. In order to estimate the equilibrium effects on the twisting of bianthryl in acetonitrile, the potential of mean force $V_{\mathrm{pmf}}(\phi)$ was computed for each of the three electronic states for comparison with the intrinsic (gas phase) torsional potential $V_{\mathrm{mol}}(\phi)$.

The nonequilibrium torsional dynamics of BA following the electronic excitation was simulated in the following manner. First, 151 configurations containing the solute plus solvent coordinates and velocities were chosen from the 150 ps simulation of ground state bianthryl in acetonitrile. These 151 coordinate and velocity sets, corresponding to the ground state equilibrium distribution, provided the initial conditions for the nonequilibrium trajectories. For each nonequilibrium trajectory, the BA molecular mechanics torsional potential and the partial atomic charges were instantaneously switched from the S_0 state to the LE or CT state. Then the system was propagated forward in time for 2 ps by integrating the equations of motion. Thus, the simulations of the torsional dynamics of bianthryl in acetonitrile on the LE and CT surfaces each consisted of 151 trajectories with different initial conditions. The nonequilibrium torsional distributions were constructed at selected points in time (0.5, 1, 1.5, 2 ps) following the simulated excitation from the instantaneous values of the BA torsional coordinate observed in the set of 151 trajectories.

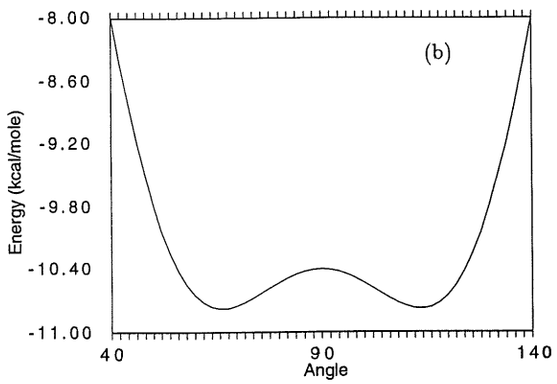

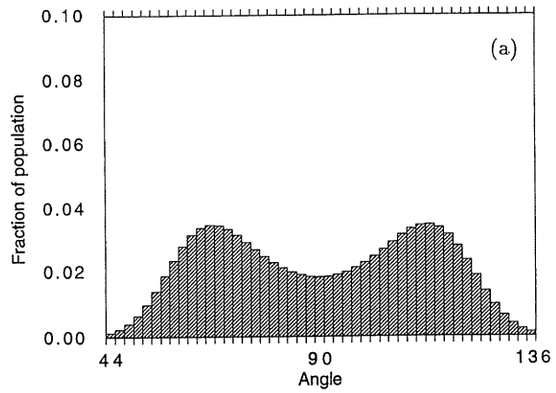

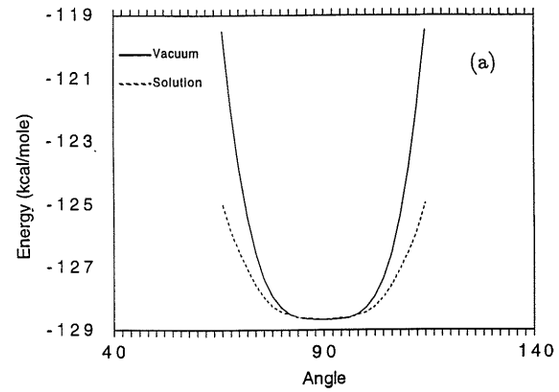

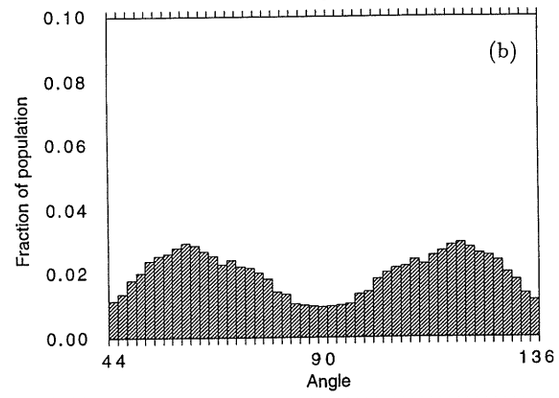

Fig. 2. Torsion potential of Yamasaki et al. in kcal/mol. (a) S_0 state, solid line is Yamasaki's potential, the dashed line is the solvent modified potential as determined through the use of the torsion distributions. (b) S_1 state.

3. Results and discussion

The ground state torsional potential of mean force for BA in acetonitrile is compared with the vacuum potential in fig. 2. The vacuum potential is flat near the equilibrium angle but rises steeply as the twist angle increases beyond 110° (70°). In solvent, the appearance of the ground state torsional potential is similar, but with decreased curvature. The minimum is located at $\phi_{eq}=90°$ in vacuum and in solvent. The root mean square fluctuation of the torsional coordinate is calculated to be $\langle(\Delta\phi)^2\rangle^{1/2}=6.6°$ and $\langle(\Delta\phi)^2\rangle^{1/2}=8.0°$ in vacuum and in acetonitrile, respectively.

The equilibrium results obtained from the bianthryl trajectories on the LE and CT potentials are shown in figs. 3 and 4. The solvent modified bianthryl dihedral angle distributions for LE and CT are compared with the Boltzmann distribution on the vacuum potential surface in fig. 3 and the corresponding potentials of mean force are shown in fig. 4. The most pronounced effect of the acetonitrile sol-

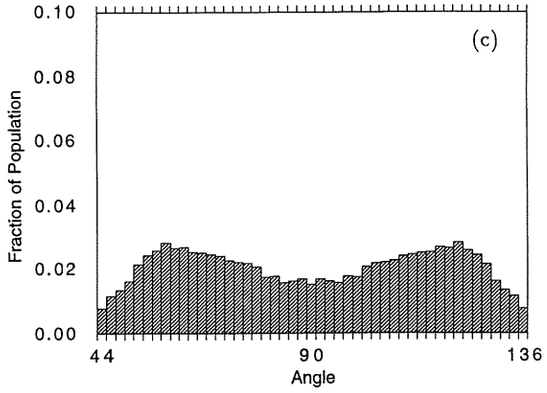

Fig. 3. Distribution of the central dihedral angle. (a) Excited torsion in a vacuum. (b) The LE state in solution. (c) The CT state in solution.

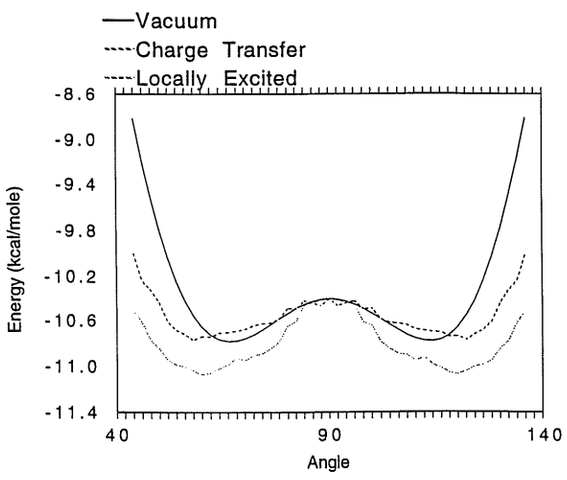

Fig. 4. Solvent modified and gas phase torsional potentials for excited bianthryl.

vent on the excited state is to increase the average twisting of BA. In the gas phase, the most probable twist angle is $\phi_{eq}=66°$ ($+114°$), while in polar solution the most probable value is 58°–60° (120°–122°). The equilibrium fractional population of conformers twisted by more than 30° away from the ground state geometry is only 16% in the gas phase, while in acetonitrile, it is 39% and 33% for the LE and CT states, respectively. The largest twist angle changes observed during the trajectories on the LE and CT states in solution were $\Delta\phi=74.7°$ (LE trajectories) and $\Delta\phi=66.2°$ (CT trajectories). The bianthryl model with CT charges has a flatter distribution of torsion angles than either the vacuum distribution or the distribution corresponding to the LE state in acetonitrile. The solvent modified effective potentials are compared in fig. 4. The minimums in the potentials of mean force are shifted to larger twist angles in solution. At the largest angle shown in fig. 4 ($\phi=123°$), the acetonitrile solvent stabilizes the twisted geometry by about 1.5 kcal/mol with respect to the gas phase potential. The barrier height increases to 0.7 kcal/mol in the LE state, a significant increase relative to the experimentally determined gas phase value ($\approx$0.4 kcal/mol). However, the computed barrier in the CT state remains virtually unchanged from the gas phase value.

Recent experimental data by Wortmann et al. [26] support the computed results obtained for the LE state in solution. From a determination of the S_1 torsional potential of BA in the nonpolar solvent 2-methylbutane, it was found that the minimum in S_1 moved to $\phi_{eq}=62°$ (118°) from its gas phase value of $\phi_{eq}=70°$ (110°). Furthermore, the barrier height at $\phi=90°$ increased to 255 cm^{-1} (0.73 kcal/mol) in solution, more than doubling in value compared to their estimated gas phase value of 116 cm^{-1} (0.33 kcal/mol). The experimental data pertain to the LE state, since only a very small fraction of the BA molecules can be expected to be in the CT state in this particular solvent. Although the solvents employed experimentally and computationally are different, the measured and computed changes in ϕ_{eq} ($\Delta\phi\approx8°$) and in the barrier height ($\approx$0.3–0.4 kcal/mol) are nearly identical. This suggests that, at least for the LE state of BA, the solvent effect on the torsional potential may be attributed to nonspecific effects related to solvent size (e.g. both acetonitrile and 2-methyl butane are bulky solvents) rather than specific solute–solvent interactions.

It should be noted that a variety of semiempirical electronic structure methods (HMO [27], QCFF/PI [25], AM1 [28]) all predict a very steeply increasing gas phase LE potential below (above) $\phi=55°$ (125°) due to rising steric interactions between the hydrogens of the two anthracene moieties. Twist angles far outside this range cannot be expected to occur often as a result of solvent interactions, because of the intrinsic barrier, although we have not carried out electronic structure calculations to optimize the torsional potential at very large twist angles.

The time evolution of the BA torsional distribution functions calculated from the nonequilibrium trajectories in acetonitrile following the simulated excitation to the LE and CT states are shown in figs. 5 and 6, respectively. The data is very noisy even when averaged over 151 trajectories. Still, the "flow" of the distribution functions from the ground state distribution towards the equilibrium excited state populations can be clearly seen in both sets of trajectories. At 0.5 ps after the simulated excitation, the torsional populations still have a Gaussian shape characteristic of the ground state; by 1 ps after the excitation, the bimodal features of the excited state distribution functions are apparent. At 2 ps following the simulated excitation, the wings of the distribution corresponding to the most twisted conformations are sub-

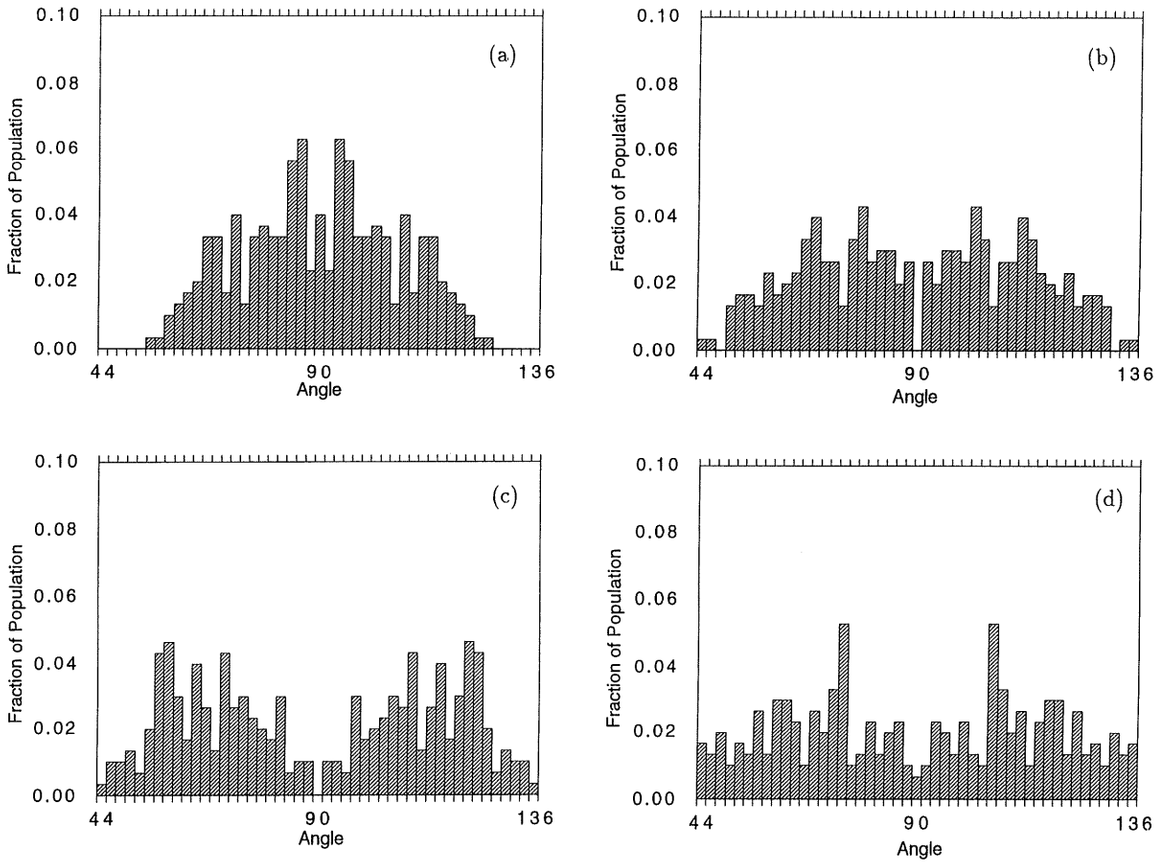

Fig. 5. Time evolution of bianthryl torsion distribution after excitation to the LE state at (a) 0.5 ps, (b) 1.0 ps, (c) 1.5 ps, (d) 2.0 ps.

stantially filled in. Qualitatively, the twisting dynamics appears to occur on the same time scale on both the LE and CT surfaces; although from the comparison of the nonequilibrium torsional distribution functions at 1.5 ps following excitation, it looks as if the relaxation is slightly faster on the LE surface. The relaxation time τ_t for bianthryl on the torsional surface is thus estimated to be between 1.5 and 2 ps in acetonitrile. It is perhaps surprising that the torsional relaxation times on the two surfaces are so similar considering that the CT state is expected to be much more strongly coupled to the polar solvent, and dielectric friction should slow down the twisting dynamics. We attribute the relatively small charge effect on the twisting dynamics to two factors: (1) the delocalization of the charge in the CT state over a large molecular region, and (2) the very fast solvation relaxation (τ_s) of acetonitrile. This is discussed below.

The atomic charges in our simulated CT state correspond to a fully developed zwitterionic state with transfer of an entire electron. However, about 55% of the net change in charge is spread out rather than being localized on just a few atoms. Seemingly large buildups (depletions) occur on C9 (C9′) and C10 (C10′) which accept (donate) approximately 0.25 and 0.20, respectively, of the transferred electronic charge. However, C9 and C9′ are interior atoms partially shielded from the solvent, so these charge changes will not be felt strongly by the solvent. Furthermore, these four atoms all lie on the central symmetry axis and hence the changes in solute–solvent interactions caused by the charge perturbation upon excitation will tend not to introduce any torque on

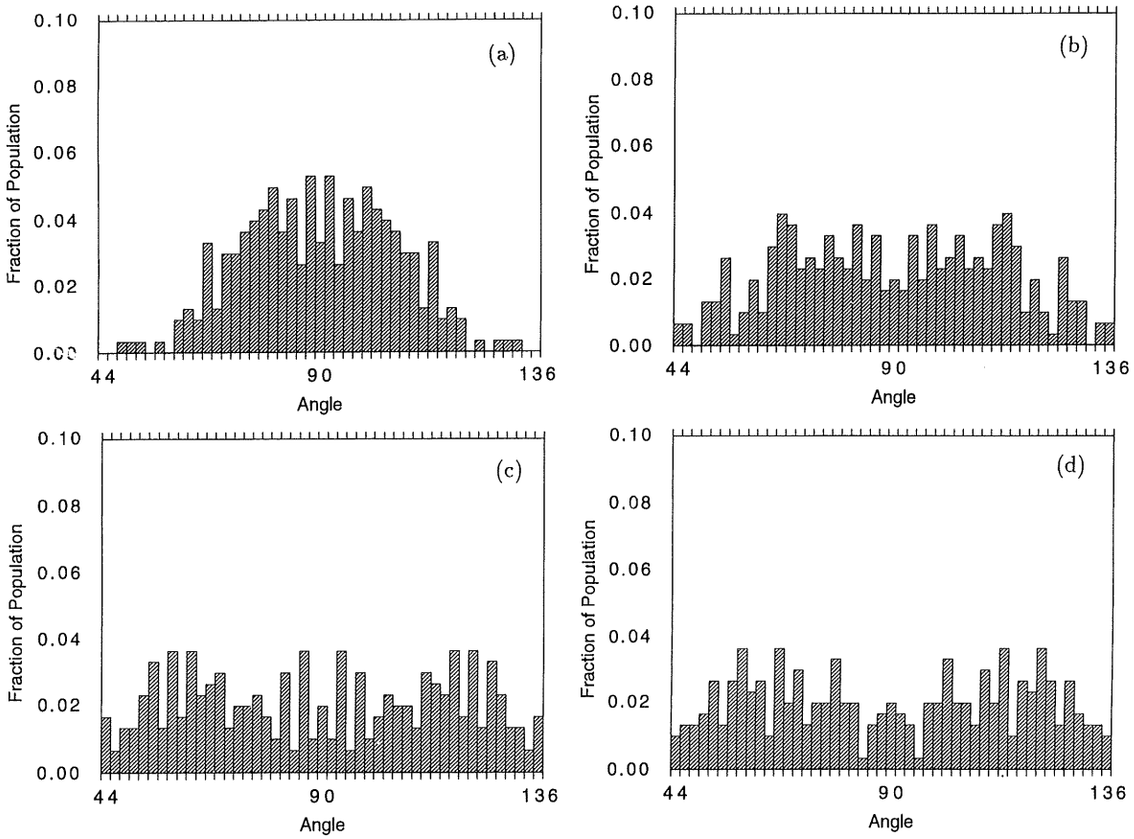

Fig. 6. Time evolution of bianthryl torsion distribution after excitation to the CT state at (a) 0.5 ps, (b) 1.0 ps, (c) 1.5 ps, (d) 2.0 ps.

the molecular propeller planes. Thus, the twisting relaxation on the CT surface may not be significantly influenced by the polarity of the state and hence it relaxes essentially at the rate of the LE state.

In fig. 7, we show the autocorrelation function for the fluctuations in solute–solvent interaction energy. The relaxation of this correlation function defines, within the framework of linear response theory, the "solvation time" of the liquid τ_s. While as defined, τ_s depends on the probe, experimentally (the relaxation of time dependent Stokes shifts) τ_s is found to be relatively independent of the probe for many liquids [7,10–12]. Several simulations of spherical solutes [29–31], ion pairs [32–34], and polyatomic solutes [35–37] in water have reported solvation times. A very complete study of the solvation dynamics of monatomic ions in acetonitrile has been recently reported by Maroncelli [38]. In both water and acetonitrile, τ_s is on the order of a few hundred femtoseconds. The shape of the bianthryl–acetonitrile solvation correlation function (fig. 7) is characteristic of the early and dominant portion of the decay observed in the simulations of ions in acetonitrile, although in the ionic simulations an additional small amplitude component appears which is not present in fig. 7. Small amplitude motions of the acetonitrile molecules in the first solvation shell of the bianthryl provide the major mechanism for the relaxation.

The time scale for acetonitrile relaxation following a charge perturbation, τ_s, is almost an order of magnitude faster than the time scale for the twisting of bianthryl, τ_t, following the simulated excitation onto the excited state potential. Extensive rearrangement of the solvent is required to accommodate the twist-

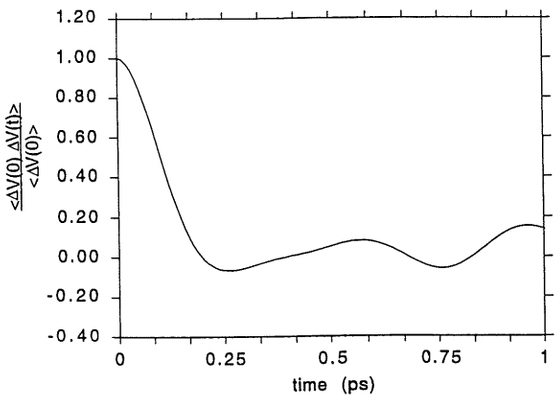

Fig. 7. Normalized autocorrelation function for the fluctuation in the electrostatic solute–solvent interaction energy, $\langle \Delta V(0)\, \Delta V(t) \rangle / \langle \Delta V(0) \rangle$.

ing of this spatially extended solute molecule. Since the solvent is able to adjust much more rapidly to changes in the electrostatic potential of BA than to conformational changes, the time required for equilibration of the torsional coordinate on the LE and CT states following excitation is similar.

The question remains as to the possible role of twisting in the electron transfer dynamics of BA. Our key finding is that the twisting is much slower than the solvation time, $\tau_t > \tau_s$. The solvent fluctuations (and hence τ_s) will play a significant role in controlling the electron transfer because the solvent modulates the energy gap between S_0 and S_1 (the adiabatic mixture of LE and CT) and hence the coupling between the states. However, qualitatively we expect some fraction of the BA molecules remains unreactive on the ultrafast solvation time scale, because the twist angle for this population remains very close to 90° where the electronic coupling between the rings is minimal. This population would have to twist further away from the ground state geometry before reacting. This picture predicts a biexponential decay curve of the LE excited state. The initial electron transfer is determined by the ultrafast solvent fluctuations around those BA monomers with conformations predisposed to facilitate electron transfer, while the slower portion of the decay reflects the twisting of the initially unreactive molecules.

Barbara and co-workers [9,39] have developed a kinetic model for electron transfer in bianthryl which fits their experimental fluorescence data well. The interesting feature of the time resolved emission spectra of BA is the persistence of a peak in the emission spectrum from the LE state as emission from the CT state grows in. To account for this observation, these authors have postulated a small barrier in the adiabatic free energy surface S_1 between an LE-like state and a CT-like state. Such a model reproduces the emission spectrum without considering the effect of twist angle on the electron transfer dynamics. Alternatively, the delayed twisting of the initially unreactive ($\phi \approx 90°$) monomers could also account for the presence of LE emission as the CT emission grows in.

To further address the question of the possible role played by conformational dynamics in excited state electron transfer in BA and related TICT molecules, better estimates are needed of the dependence of the coupling matrix elements on twist angle. If it is found that there is a large variation in the coupling with twist over the range of twist angles accessible to the molecule in the excited state, it would be useful to develop kinetic models for the electron transfer which include the twisting dynamics explicitly, given our observation that the twisting occurs on a slower time scale than the solvation time.

Acknowledgement

This work has been supported by grants from the National Science Foundation (DMB 9105208) and the National Institutes of Health (GM-30580). We acknowledge the Pittsburgh Supercomputer Center for a grant of computer time. We thank J.D. Westbrook for assistance with the electronic structure calculations.

References

[1] P.F. Barbara and W. Jarzeba, Advan. Photochem. 15 (1990) 1.
[2] W. Rettig, Angew. Chem. Intern. Ed. Engl. 25 (1986) 971.
[3] E. Lippert, W. Lüder and H. Boos, in: Advances in molecular spectroscopy, ed. A. Mangini (Pergamon Press, Oxford, 1962) p. 443.
[4] A. Subaric-Leitis, C. Monte, A. Roggan, W. Rettig, P. Zimmerman and J. Heinze, J. Chem. Phys. 93 (1990) 4543.

[5] L.R. Khundkar and A.H. Zewail, J. Chem. Phys. 84 (1986) 1302.
[6] K. Yamasaki, K. Arita, O. Kajimoto and K. Hara, Chem. Phys. Letters 123 (1986) 277.
[7] P.F. Barbara and W. Jarzeba, Accounts Chem. Res. 21 (1988) 195.
[8] E. Lippert, W. Rettig, V. Bonačić-Koutecký, F. Heisel and J.A. Miehe, Advan. Chem. Phys. 68 (1987) 1.
[9] T.J. Kang, W. Jarzeba, P. Barbara and T. Fonseca, Chem. Phys. 149 (1990) 81.
[10] M. Maroncelli, J. MacInnis and G.R. Fleming, Science 243 (1989) 1674.
[11] M.A. Kahlow, T.J. Kang and P.F. Barbara, J. Phys. Chem. 91 (1987) 6452.
[12] J.D. Simon, Accounts Chem. Res. 21 (1988) 128.
[13] A. Warshel and M. Karplus, Chem. Phys. Letters 32 (1975) 11.
[14] R.R. Birge and L.M. Hubbard, J. Am. Chem. Soc. 102 (1980) 2195.
[15] I. Ohmine, J. Chem. Phys. 85 (1986) 3342.
[16] L.R. Pratt and D. Chandler, J. Chem. Phys. 67 (1977) 3683.
[17] R.M. Levy, M. Karplus and J.A. McCammon, Chem. Phys. Letters 65 (1979) 4.
[18] W.L. Jorgensen, R.C. Binning Jr. and B. Bigot, J. Am. Chem. Soc. 103 (1981) 4393.
[19] D.B. Kitchen, F. Hirata, J.D. Westbrook, R.M. Levy, D. Kofke and M. Yarmush, J. Comput. Chem. 11 (1990) 1169.
[20] H.C. Andersen, J. Comput. Phys. 52 (1983) 24.
[21] W.L. Jorgensen and J.M. Briggs, Mol. Phys. 63 (1988) 547.
[22] J.E. Ridley and M.C. Zerner, Theoret. Chim. Acta 32 (1973) 111.
[23] J.D. Westbrook and K. Krogh-Jespersen, ESPPAC (Excited States Properties PACkage), Rutgers University (1989).
[24] J.D. Westbrook, R.M. Levy and K. Krogh-Jespersen, J. Comput. Chem. 13 (1992) 979.
[25] W. Rettig and M. Zander, Ber. Bunsenges. Physik. Chem. 87 (1983) 1143.
[26] R. Wortmann, K. Elich, S. Lebus and W. Liptay, J. Chem. Phys. 95 (1991) 6371.
[27] F. Schneider and E. Lippert, Ber. Bunsenges. Physik. Chem. 74 (1970) 624.
[28] K. Krogh-Jespersen, unpublished results.
[29] M. Rao and B.J. Berne, J. Phys. Chem. 85 (1981) 1498.
[30] M. Maroncelli and G.R. Fleming, J. Chem. Phys. 89 (1988) 5044.
[31] O.A. Karim, A.D.J. Haymet, M.J. Banet and J.D. Simon, J. Phys. Chem. 92 (1988) 3391.
[32] J.S. Bader and D. Chandler, Chem. Phys. Letters 157 (1989) 501.
[33] E.A. Carter and J.T. Hynes, J. Phys. Chem. 93 (1989) 2184.
[34] S.B. Zhu, J. Lee, J.B. Zhu and G.W. Robinson, J. Chem. Phys. 92 (1990) 5491.
[35] R.M. Levy, D.B. Kitchen, J.T. Blair and K. Krogh-Jespersen, J. Phys. Chem. 94 (1990) 4470.
[36] J.D. Westbrook, R.M. Levy and K. Krogh-Jespersen, Proc. SPIE Intern. Soc. Opt. Eng. 1640 (1992) 10.
[37] P.L. Munro, D. Harris, J. Bennyhill, B. Hudson and P.R. Callis, Proc. SPIE Intern. Soc. Opt. Eng. 1640 (1992) 240.
[38] M. Maroncelli, J. Chem. Phys. 94 (1991) 2084.
[39] K. Tominaga, G.C. Walker, T.J. Kang, P.F. Barbara and T. Fonseca, J. Phys. Chem. 95 (1991) 10485.